
The Eurasia Proceedings of Science, Technology, Engineering & Mathematics (EPSTEM)

Volume 1, Pages 158-177

ICONTES2017: International Conference on Technology, Engineering and Science

OPTIMUM CFRP LENGTH FOR THE HOGGING MOMENT ZONE (HMZ) OF CONTINUOUS RC T-BEAMS

Mohammad Mohie Eldin
Beni-Suef University

Ahmed M. Tarabia
Alexandria University

Rahma F. Hasson
Sirte University

Abstract: Carbon fiber reinforced polymer (CFRP) laminates were proved as very effective method for either repairing or strengthening of used structures. However, the literature has no enough information about the behavior of RC continuous (two-span) T-section beams strengthened with CFRP laminates, especially in hogging moment zone (HMZ). This paper examines the effect of CFRP laminates lengths, used for strengthening of the hogging moment zone, upon the behavior of such beams, to determine the optimum strengthening length. 3-D theoretical models using the Finite Element (FE) Package ANSYS are used. The paper contains the main details of the FE modeling process; used element types, material properties, meshing, yield criterion and boundary conditions. The results of the proposed FE model were compared with those of a previous experimental research and very good agreement was found between both FE and experimental results. Three parameters were used in the parametric study; CFRP length, CFRP thickness, percentage ratio of the steel reinforcement (different diameters for reinforcement steel bars). To examine the effect of changing CFRP strengthening lengths, different types of results for the proposed parametric study were obtained for better understanding of behavior. Adding to this, these results were compared and analyzed at different stages of loading between first cracking of the RC studied T-beams and their failure. These results include load-deflection curves, bending moment diagrams, stresses and strains of the CFRP laminates, stresses and strains of steel reinforcement bars, redistribution of moments, energy dissipation, ductility, shear (bond) stresses and failure modes of the studied beams. It can be concluded that changing CFRP length in the HMZ is very effective upon the overall behavior of T-section continuous RC beams. This effect begins after first crack and considered as effective after the yielding of upper steel bars. Increasing the lengths of CFRP laminates increases capacity, ductility and energy dissipation of strengthened beams in the hogging moment zone. Also, it improves utilizing of upper steel bars and redistribution of moments between sagging and hogging moments. Practically, Design-Codes of using CFRP in strengthening of structures concern only with both CFRP strengthening length and its corresponding anchorage length. As a result, definitions of both optimum CFRP strengthening length and CFRP anchorage length were expressed. Finally, criteria to calculate both of them were concluded.

Keywords: ANSYS, CFRP, optimum length, rc beam, t-beam

Introduction

Only little literature is available considering the behavior of two-span continuous beams with rectangular sections strengthened using CFRP laminates. Experimentally, an external strengthening using CFRP laminates was found to increase the load capacity of such beams. Also, moment redistribution in such beams is possible if the longitudinal and transverse reinforcement configuration is chosen properly [1]. Increasing the number of CFRP layers, not beyond its optimum value, increases both flexure and shear strength and capacity. However, it decreases ductility, moment redistribution, and ultimate strain on CFRP laminates [2, 3, and 12]. Extending the CFRP length to cover the entire hogging or sagging zones did not prevent peeling failure of the CFRP laminates

- This is an Open Access article distributed under the terms of the Creative Commons Attribution-Noncommercial 4.0 Unported License, permitting all non-commercial use, distribution, and reproduction in any medium, provided the original work is properly cited.

- Selection and peer-review under responsibility of the Organizing Committee of the conference

*Corresponding author: Mohammad Mohie Eldin- E-mail: mohammad_mohie_eldin@yahoo.com

[2]. It was shown that the debonding mechanisms are governed by shear forces and moment redistribution occurring in multi-span beams [14]. Adding to thickness of CFRP laminates and strengthening of both hogging and sagging regions, end anchorage techniques are effective upon the response of reinforced high strength concrete (RHSC) continuous beams [3]. It was shown that externally strengthened RC beams with bonded CFRP laminates have significant increases in their ultimate loads [4]. CFRP strengthened cross-sections restrict the rotation of plastic hinges at their locations, and allow additional plastic hinges formation in unstrengthened cross-sections [14]. Also, Saribiyik et al [5] conducted that wrapping methods of CFRP laminates affect the behavior of strengthened beams in terms of flexural strength, ductility and energy absorption capacity. On the other side, T-section beams are very important since it takes into account the interaction between both beams and slabs. However, very rare research is available about T-section simple or continuous beams strengthened using CFRP laminates. Rahman et al [6] presented an effective technique of applying CFRP laminate for strengthening the hogging zone of continuous T beam considering column constrains. The purpose of this paper is to investigate the effect of CFRP laminates lengths upon strengthening of T-section continuous (two spans) beams in the hogging moment zone; above and around the intermediate support.

Verification of Finite Element Modeling

FE model used in this paper was verified through the beam (B2) of the experimental program made by Saleh and Barem (2013) as shown in Figures 1 and 2. CFRP laminates used in this study were at top face of beam at the hogging zone and bottom face of beam at the sagging zones. External anchorages used in this study were made from CFRP U-shape at the end of longitudinal CFRP laminates. Thickness of used CFRP laminates is 0.113 mm.

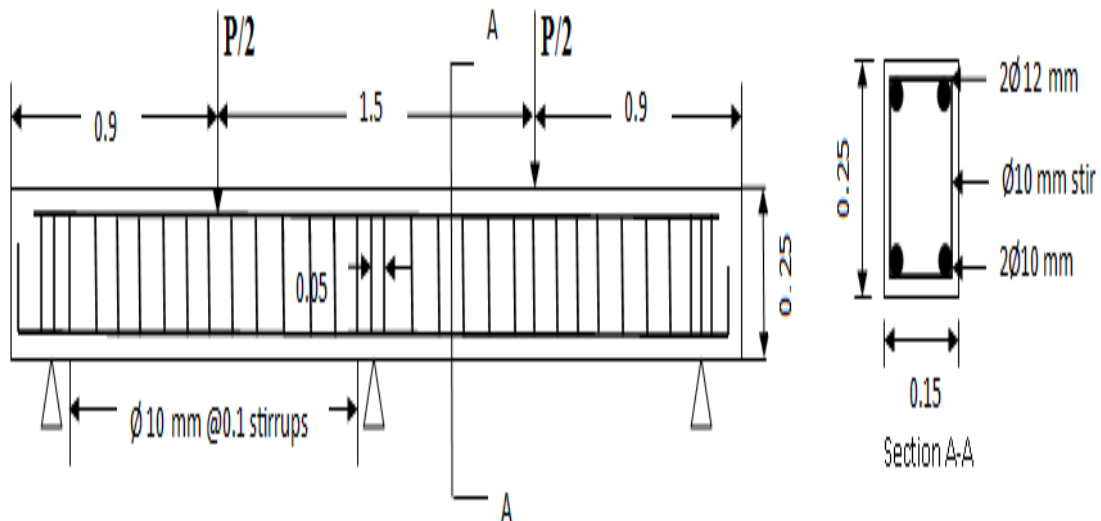


Figure 1. Details of beam (B2), barem et al [1]

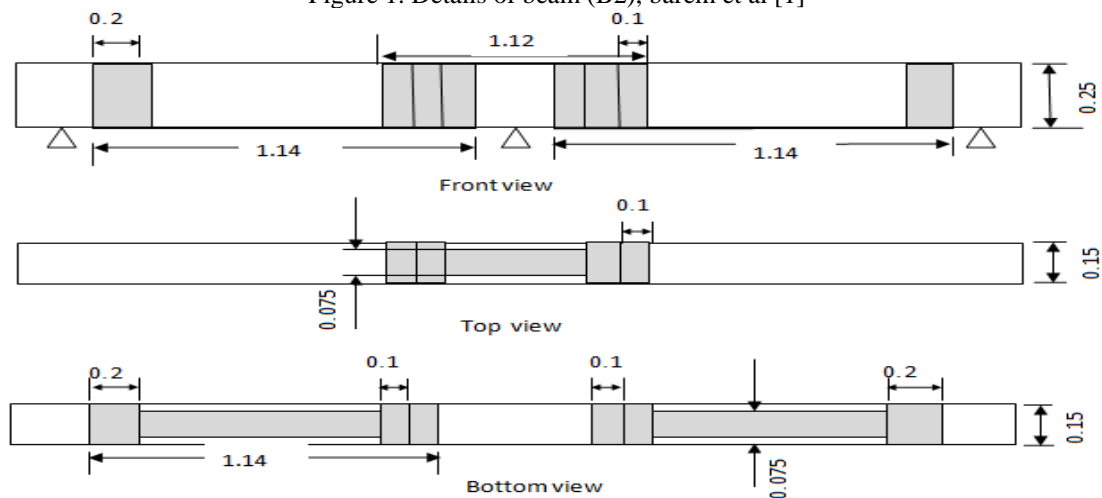


Figure 2. CFRP locations and anchors (in meters)

2.1 Element Types

Six types of finite elements that have plasticity, large deflection, and large strain capabilities are used for 3-D modeling of the tested beams. These elements are SOLID65, SOLID45, LINK180, SHELL181, CONTA173 and TARGET170, as follows:

- SOLID65 is defined by eight nodes having three degrees of freedom at each node; translations in the nodal x, y, and z directions. The solid is capable of cracking in tension and crushing in compression. It is used for modeling of concrete elements.
- SOLID45 is used for modeling of steel plates of loading and supporting. It is similar to SOLID65 but without crushing/cracking capabilities.
- LINK180 is a uniaxial tension-compression element with three degrees of freedom at each node; translations in the nodal x, y, and z directions. It is used for modeling of steel bars and stirrups.
- SHELL181 is a 4-node element with six degrees of freedom at each node; translations in the x, y, and z directions, and rotations about the x, y, and z-axes. As it can be used for layered composite, it is used for the modeling of CFRP laminates.
- CONTA173 is a 3-D contact element that is used to represent contact and sliding between “target” surface and a deformable contact surface.
- TARGE170 is a 3-D target element used to represent 3-D “target” surfaces for the associated contact elements (CONTA173). Target surface is the surface of concrete beam and the deformable contact surface is that of CFRP laminates. Both contact and target elements form “Contact Pair” which is defined as “initially bonded” to allow both sliding and gap between the two surfaces of the contact pair.

2.2 Material Properties

Table 1 shows the mechanical properties of concrete, steel reinforcement and CFRP laminates. Figure 3 shows the typical stress strain curves of concrete and CFRP, respectively, while steel is modeled using an elastoplastic curve.

Table 1. Mechanical properties of materials

Concrete (MPa)				Steel Bars (MPa)			CFRP Laminates (MPa)		
f_c	f_r	E_c	Poisson's Ratio	f_y	E_s	Poisson's Ratio	σ_{u_CFRP}	E_{CFRP}	Poisson's Ratio
30	3	26000	0.2	400	200000	0.3	3050	165000	0.33

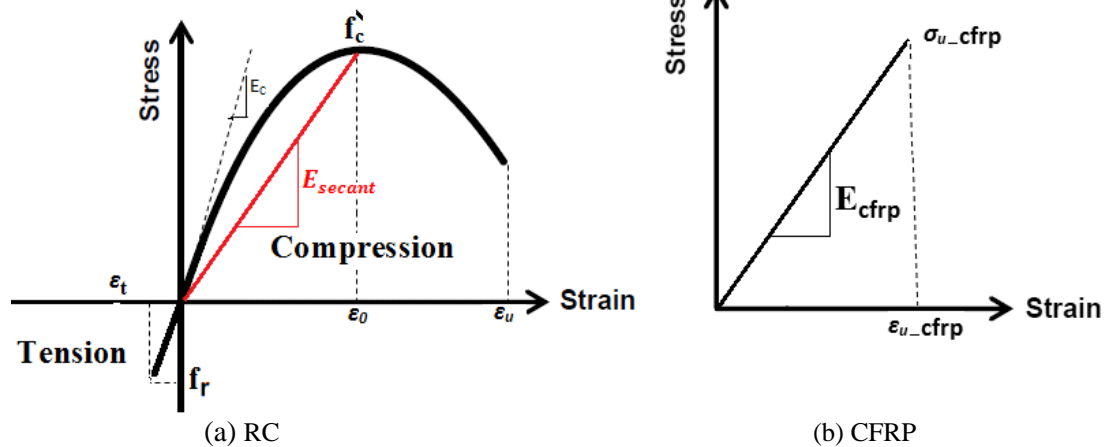


Figure 3. Typical stress-strain curves

The adhesive material is modeled using a cohesive zone model (CZM) of six major parameters; maximum normal contact stress, critical fracture energy for normal separation, maximum equivalent tangential contact stress, critical fracture energy for tangential slip, artificial damping coefficient, and flag for tangential slip under compressive normal contact stress. Since debonding occurs due to shear failure, the first two parameters were not considered. The other four parameters are 6 N/mm², 0.75 N/mm, 0.1, and 1, according to an experimental bond-slip curve [8], as shown in Figure 4.

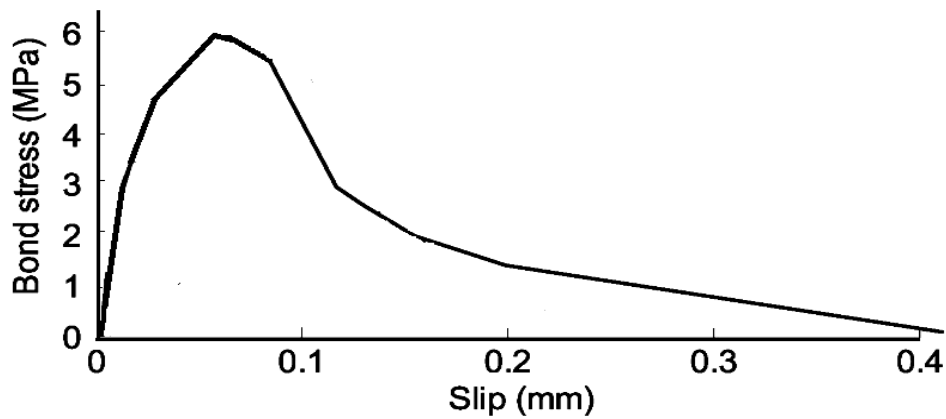


Figure 4. Local bond stress versus bond slip

2.3 Meshing

Meshing analysis was done to obtain the acceptable size of solid elements that lead to accurate results in a minimum solution time. As a result, element size of: ($x \times y \times z = 50 \times 50 \times 50$ mm) was chosen.

2.4 Boundary conditions

Outer two supports are modeled as movable supports that only allow the movement in the direction of the beam axis, while mid-support is a pinned support to prevent movement in any direction. According to symmetry, only one quarter of the beam is modeled using the suitable boundary conditions at the two planes of symmetry.

2.5 Yield Criterion

Von Mises yield criterion is used to predict the onset of the yielding, whereas the behavior upon further yielding is predicted by the ‘flow rule’ and ‘hardening law’.

2.6 Results

Figure 5 shows load vs. maximum Span-deflection of beam (B2) due both experimental and FE results. Very good agreement is achieved that insure using ANSYS as a modeling tool for continuous RC beams strengthened by CFRP laminates.

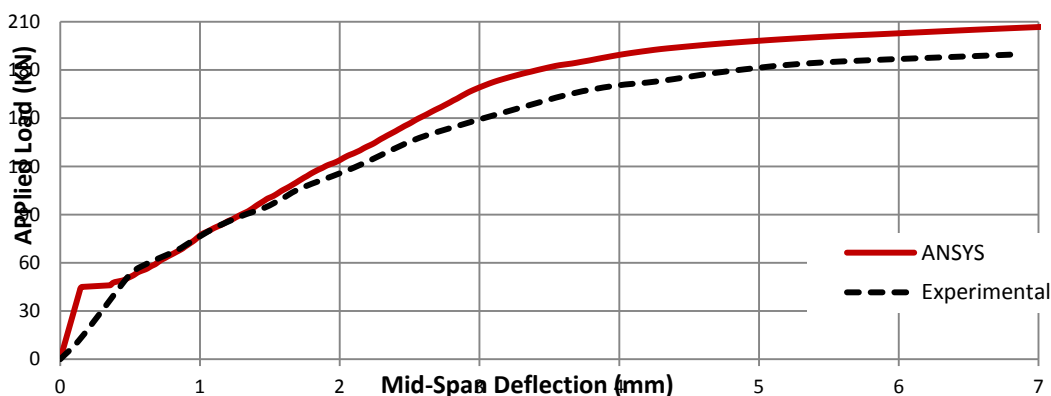


Figure 5. Results of Beam (B2), Barem et al [1]

1. Parametric Study

1.1 Dimensions and Materials of Modeled Beams

Figure 6 shows the dimensions, reinforcement, loading and CFRP pattern for strengthening of hogging moment zone (HMZ), while Figure 7 shows the corresponding bending moment diagram. ECP-203 [18] was used to design the reinforcement of the T-beam which was 4-bars- $\phi 24$ mm for the upper reinforcement in the HMZ and 4-bars- $\phi 18$ mm as lower reinforcement in the SMZ. This beam is called BC1. To allow good investigation of the effect of CFRP strengthening, the designed upper reinforcement was reduced by 75% from 4-bars- $\phi 24$ mm to 4-bars- $\phi 12$ mm, as shown in Figure 7. The thicknesses of CFRP strengthening laminates are designed using ECP-208 [19] for the T-beams with the reduced reinforcement to recover their original moment capacities either hogging or sagging. For strengthening of HMZ, CFRP thickness was designed and approximated to 0.9 mm. CFRP laminate has width equals to the web width (300 mm) and its length equals ($2L_{CFRP}$) where (L_{CFRP}) is the CFRP strengthening length per span. The mechanical properties of the materials used in the parametric study are shown in Table 1 and Figures 3 and 4.

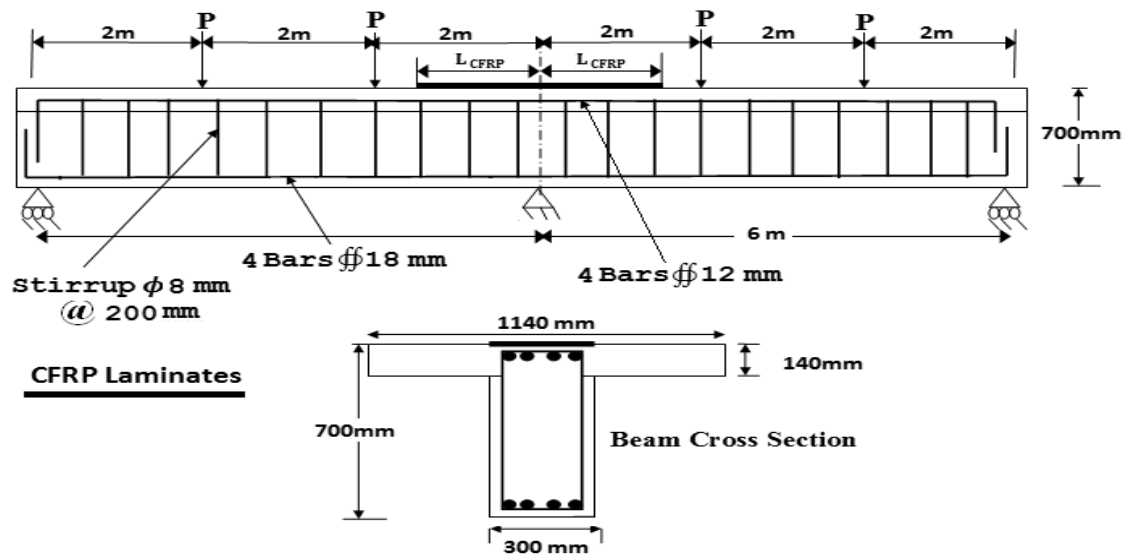
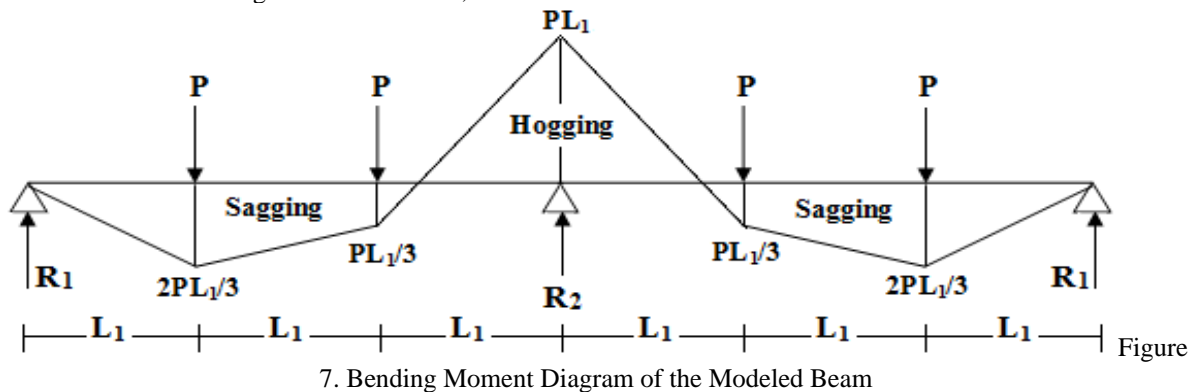


Figure 6. Dimensions, Reinforcement and CFRP Laminates in HMZ



1.2 CFRP Lengths, Loading Stages and FE Modeling

Adding to an unstrengthened (control) beam, five lengths of CFRP laminates are used to investigate the effect of CFRP strengthening length upon the behavior of beams.

These lengths are ($0.267L_{HMZ} = 400$), ($0.4L_{HMZ} = 600$), ($0.6L_{HMZ} = 900$), ($0.8L_{HMZ} = 1200$), and ($L_{HMZ} = 1500$) per each of the two spans measured from the mid-support, where L_{HMZ} is the length of the hogging moment zone (HMZ) per span. Beams were modeled in the same procedure of FE modeling mentioned in Section 2. For each beam, five loading stages were studied to analyze the behavior. These stages are:

- a. At first crack.
- b. Between first crack and steel yield.
- c. At yield of upper steel.
- d. Between steel yield and failure.
- e. At failure.

1.3 Results and Discussions

3.3.1 Load - Deflection Relation

Figure 8 shows the relation between the applied load at each span (2P) and the maximum deflection (at the point of maximum moment). The effect of strengthening appears just after first-cracking of the beams. This means that the effect of both CFRP laminates and steel bars is synchronous. Also, it is obvious that increasing CFRP length increases both capacity (maximum moment) and ductility (related to maximum deflection) of the beam.

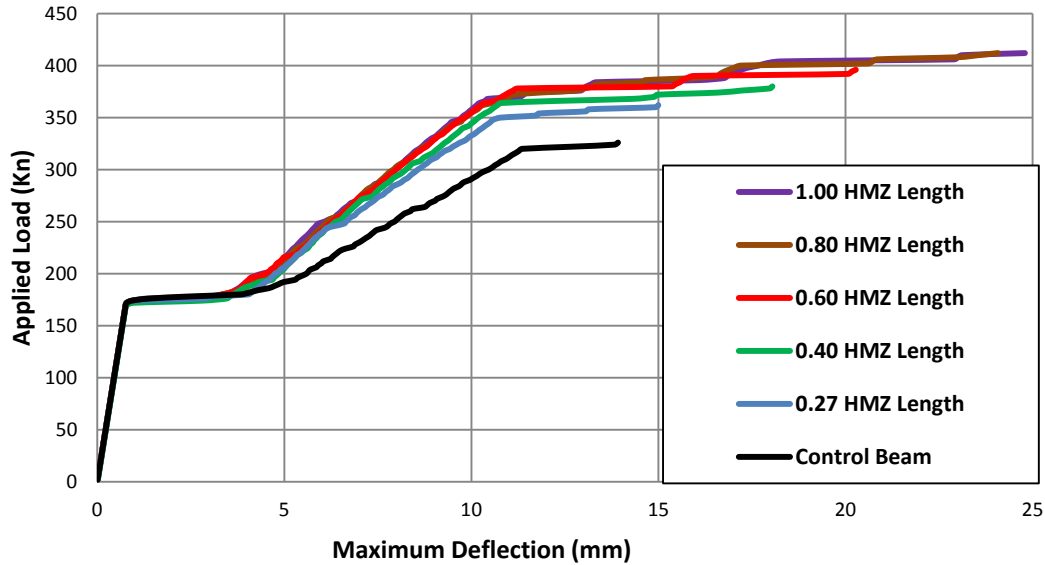


Figure 8. Load – deflection curve

Figure 9 shows the relation between maximum applied load of the beams and the ratio between CFRP length (L_{CFRP}) and length of hogging moment zone (L_{HMZ}). The relation is approximately linear till a certain length and then it is constant. This means that there is an optimum length ($L_{CFRP} = 0.8L_{HMZ}$) after which, no more improvement in the beam capacity is achieved. This length can be considered as an optimum length.

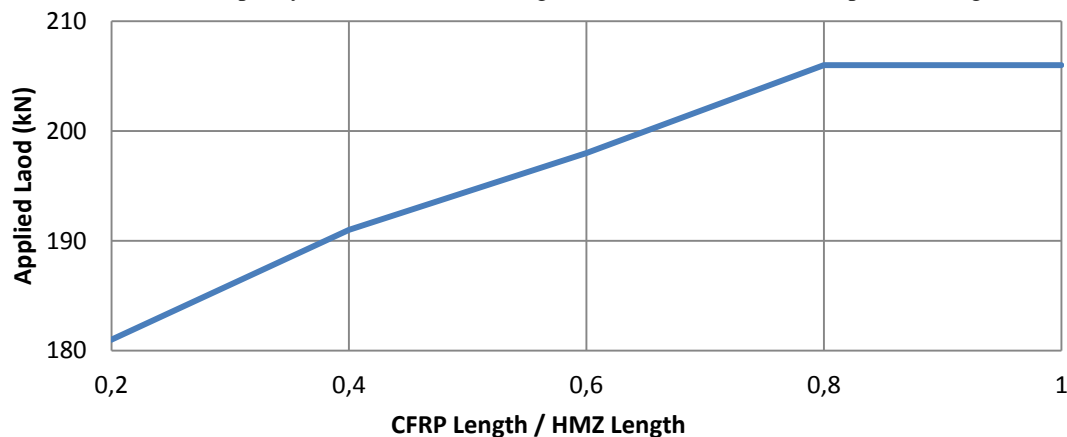


Figure 9. Load Versus (L_{CFRP}/L_{HMZ}) Ratio

3.3.2 Bending Moment Diagrams

Figure 10 shows bending moment diagrams for beams with different lengths of CFRP laminates, at failure. The shown bending moments (M_E) are calculated elastically due to applied loading at failure. According to symmetry, only one span is considered. It is shown that increasing the length of CFRP strengthening increases the capacity of the beam at hogging moment zone. Also, both diagrams of lengths ($L_{CFRP} = 0.8L_{HMZ} = 1200\text{mm}$) and ($L_{CFRP} = 1.0L_{HMZ} = 1500\text{mm}$) are very close to the degree that they seem as identical.

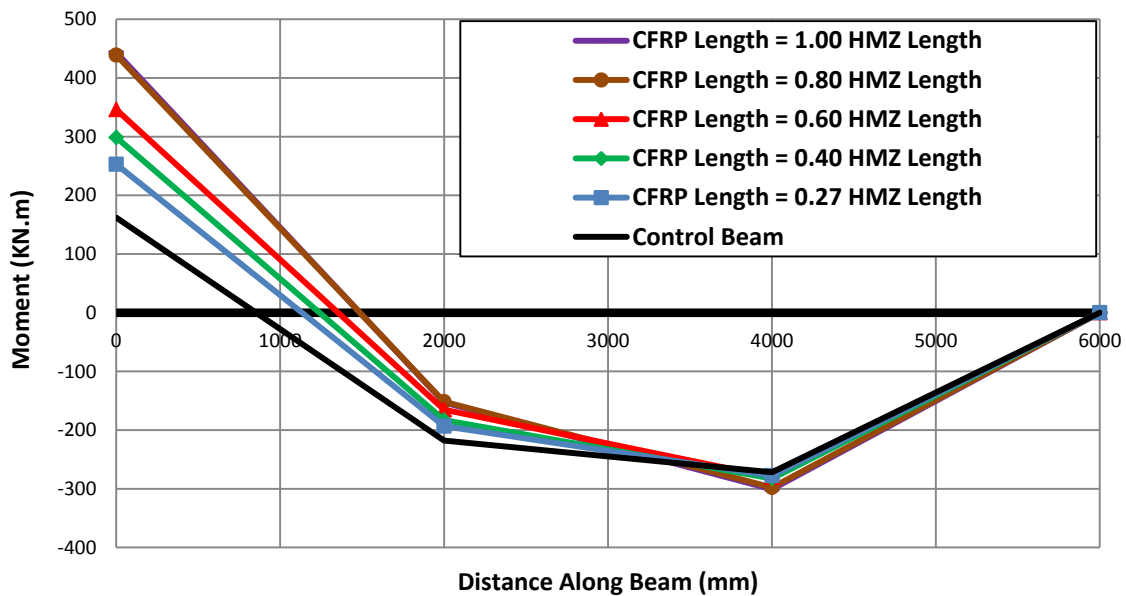


Figure 10. Bending moments at failure

3.3.3 Stresses of CFRP Laminates at Different Stages of Loadings

Figures 11 to 15 show stresses distribution of CFRP laminates along their lengths, measured from the mid-support, at the five stages of loading. Due to the elastic behavior of CFRP, strain diagrams are proportional to that of stresses and hence they are not included.

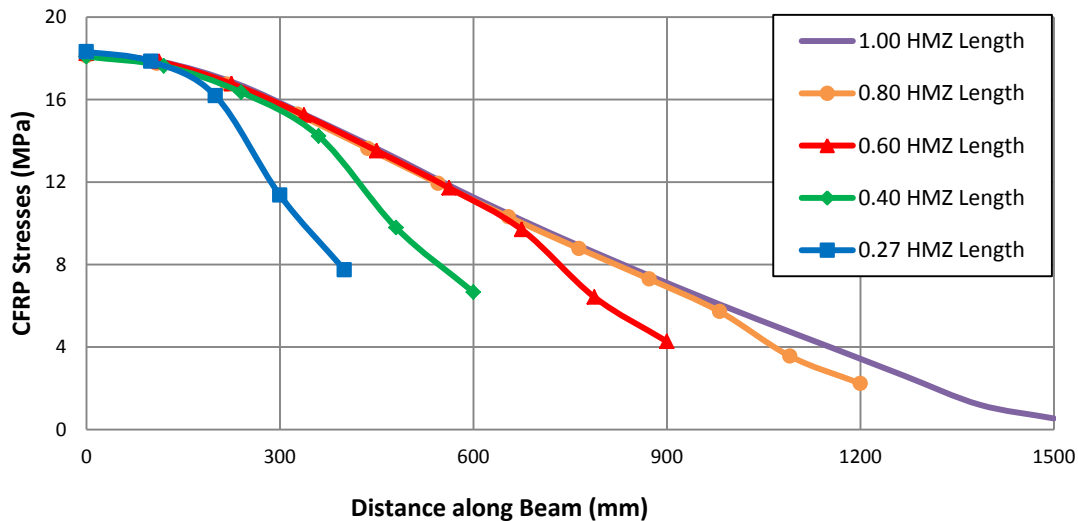


Figure 11. CFRP stresses at first crack

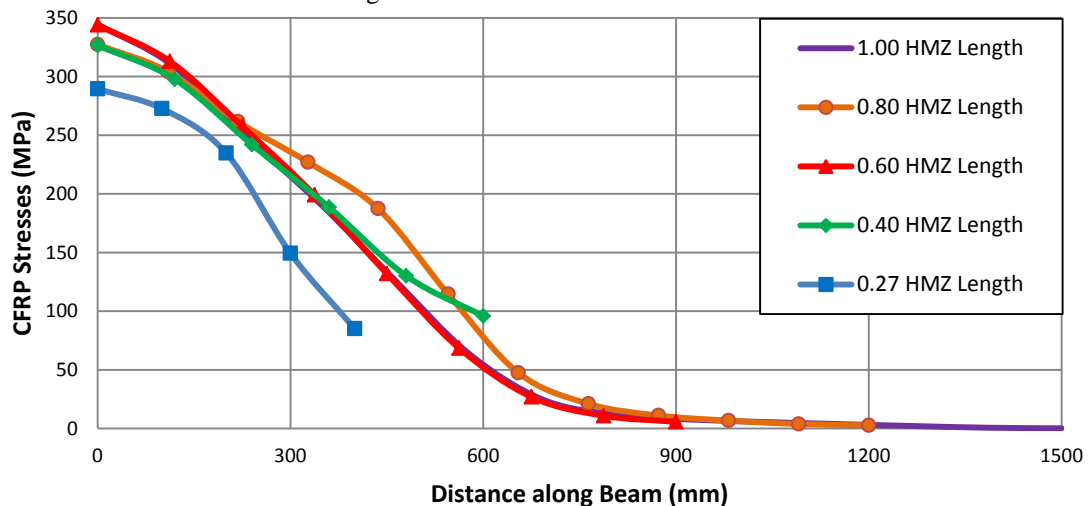


Figure 12. CFRP stresses at second stage (between first crack and upper steel yield)

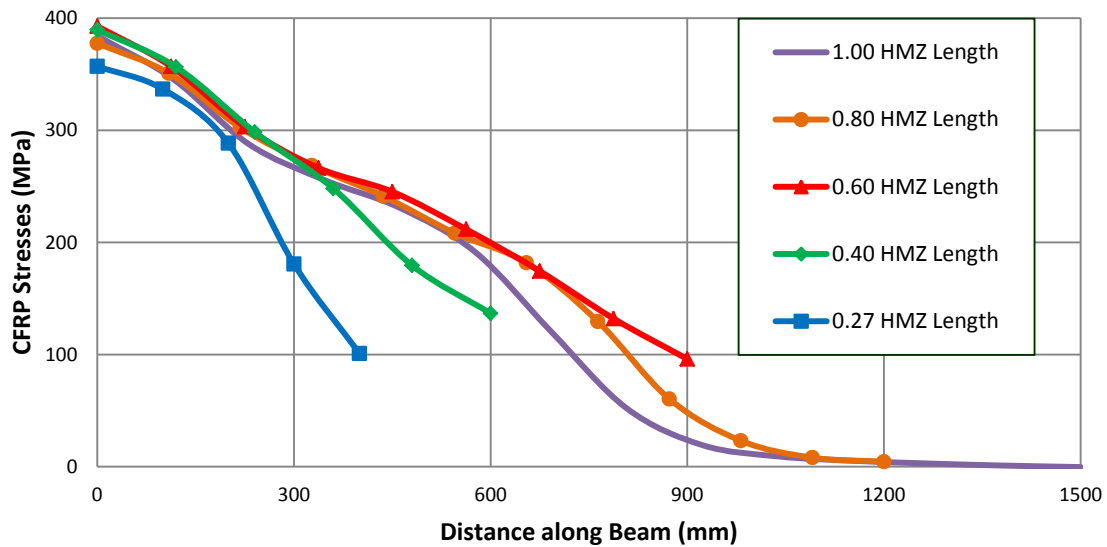


Figure 13. CFRP stresses at third stage (at upper steel yield)

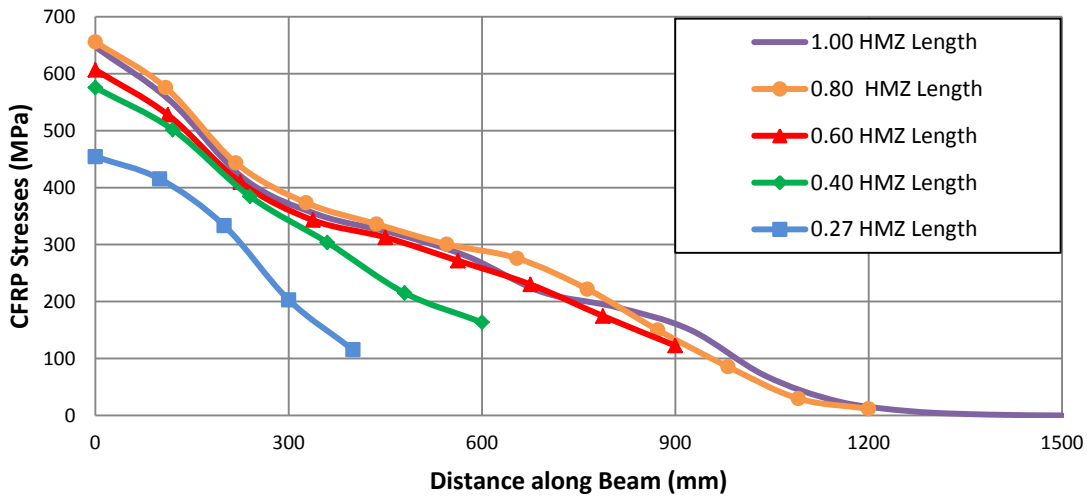


Figure 14. CFRP stresses at fourth stage (between upper steel yield and failure)

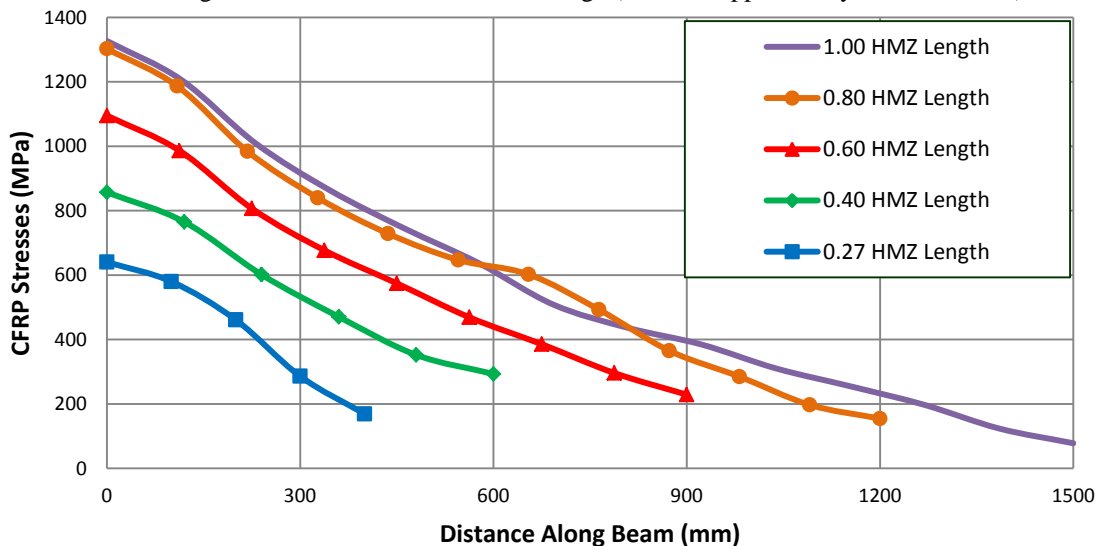


Figure 15. CFRP stresses at fifth stage (failure)

According to figures, the following may be concluded:

1. Maximum stresses (strains) lie at mid-support and decrease gradually till laminates ends.
2. Effect of strengthening with CFRP laminates begins just after the first crack of concrete.
3. Stresses in CFRP laminates become increasingly apparent and influential after yielding of upper steel bars.
4. At the same distance from the mid-support, CFRP laminates with greater lengths bear greater stresses.

5. At their ends, CFRP laminates with greater lengths have less stresses which mean that increasing CFRP laminate length decreases concentration of stresses at its end.
6. Stresses at the beginnings of CFRP laminates for both lengths 1200 and 1500 mm are very close and can be considered as equal. These stresses are the biggest comparing with other CFRP lengths.
7. According to Figures 12 to 14, stresses at the ends of CFRP laminates for both lengths 1200 and 1500 mm are approximately equal and close to zero, while this is not the case for other lengths.
8. As a conclusion, the optimum CFRP length considering the distribution of stresses/strains along CFRP length is ($L_{CFRP} = 0.8L_{HMZ}$).

3.3.4 Stresses/Strains for Each Individual CFRP Length

It was found that the behavior in all the stages of loading is the same for all the lengths. So, only the results of lengths; 600, 1200 and 1500mm (0.4, 0.8 and 1.0 HMZ Length), will be shown in Figures 16 and 17.

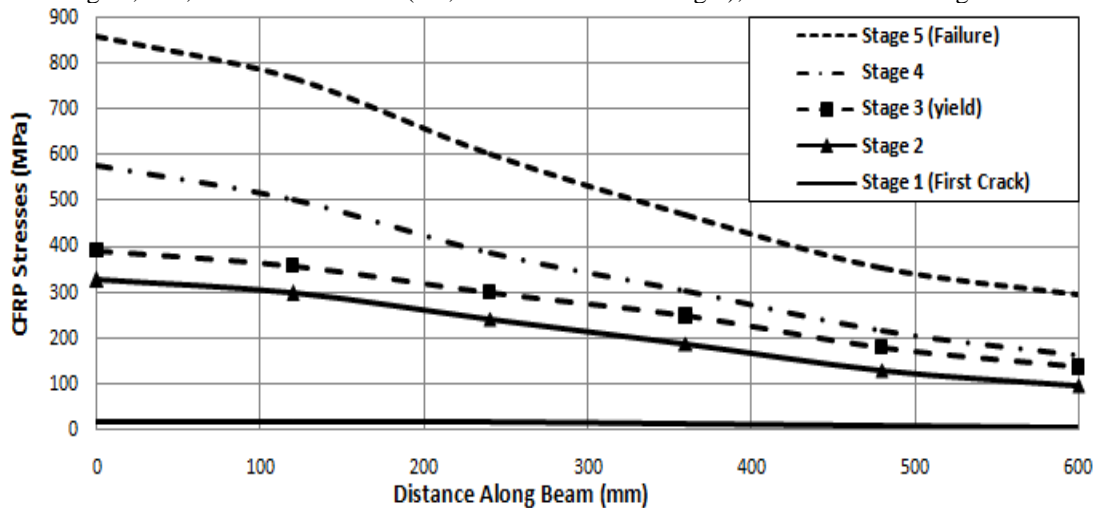


Figure 16. Stresses along CFRP length ($L_{CFRP} = 0.4 L_{HMZ}$)

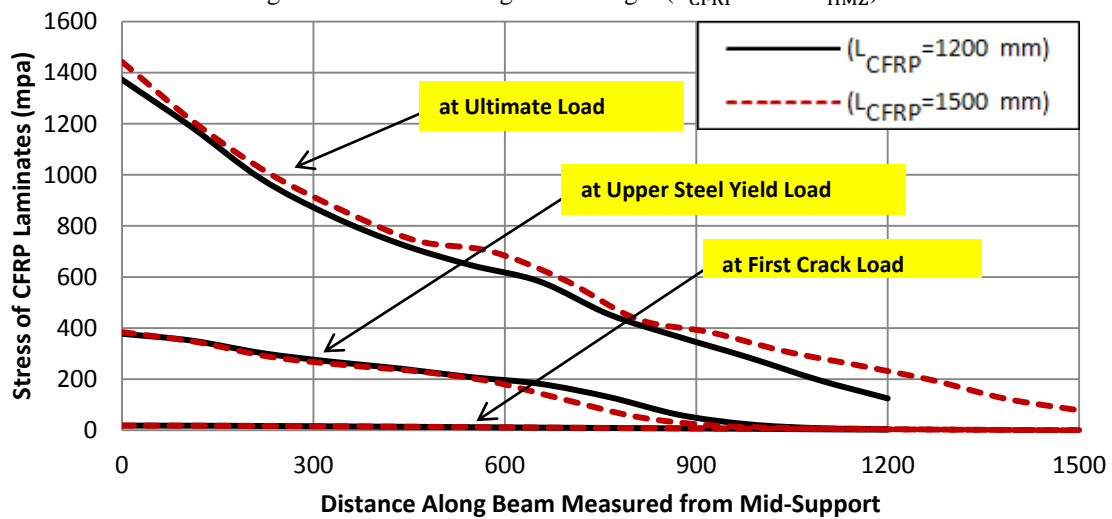


Figure 17. Stresses along CFRP ($L_{CFRP} = 0.8$ and $1.0 L_{HMZ}$)

According to results, the following may be added to what previously concluded:

1. Before steel yielding, maximum CFRP stresses, at mid supports, are less than yield stress of steel which means less utilizing of CFRP.
2. After steel yielding, increasing CFRP lengths increases their stresses beyond yield stress of steel which means more utilizing of strengthening till failure. However, this increasing will approximately vanish at a certain CFRP length ($L_{CFRP} = 0.8L_{HMZ}$).
3. Maximum contribution of the CFRP laminates in strengthening lies after yielding of steel.
4. At yielding of steel for the 1500mm-length CFRP laminate, the length of zero-stresses-part is about 500 mm which means that about 33% of the length is useless at this stage. This percentage decreases to about 16.5% in the stage (4).
5. However, at yielding of steel for the 1200mm-length CFRP laminate, the length of zero-stress-part is about 150 mm which means that only 12.5% of the length is useless. However, this percentage decreases to about zero in the stage (4).

6. The results insure that CFRP length of ($L_{CFRP} = 0.8L_{HMZ}$) is the optimum length.

3.3.5 Stresses and Strains in Upper Steel Bars at Different Stages of Loadings

Figures 18 to 20 show stresses in the upper steel bars along their lengths until steel yielding. Both stresses and strains are relative due elastic behavior of steel in these stages of loading, hence strains are not included. Figures 21 to 24 show stresses and strains for the last two stages of loading; after steel yield and till failure.

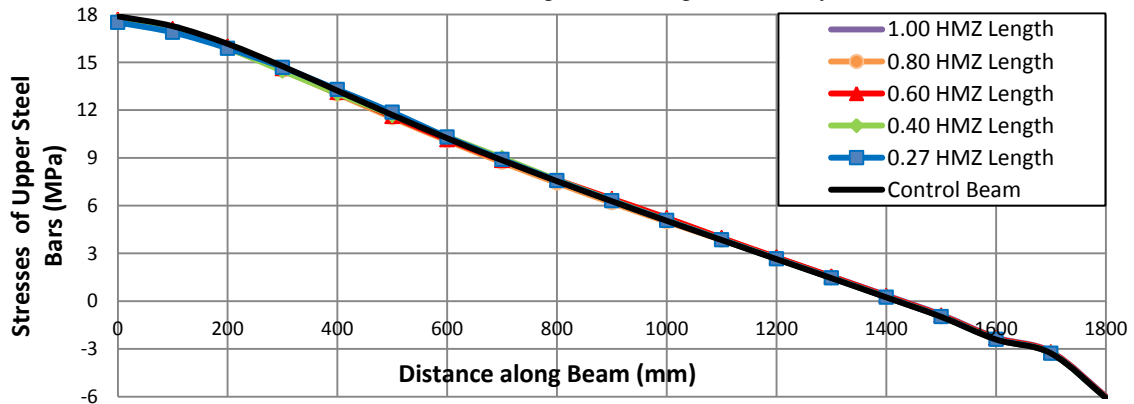


Figure 18. Stresses in upper steel bars at first crack

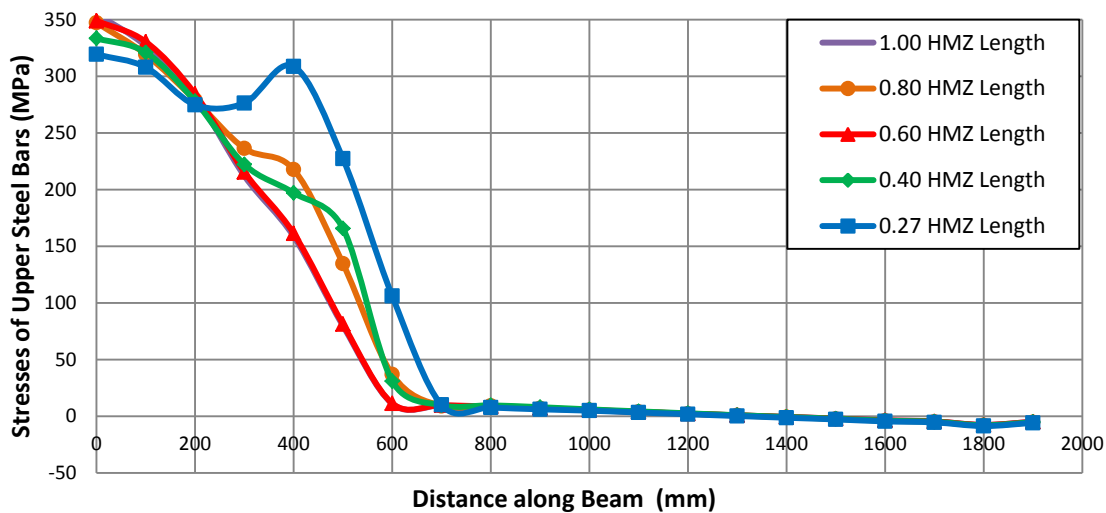


Figure 19. Stresses in upper steel bars at second stage

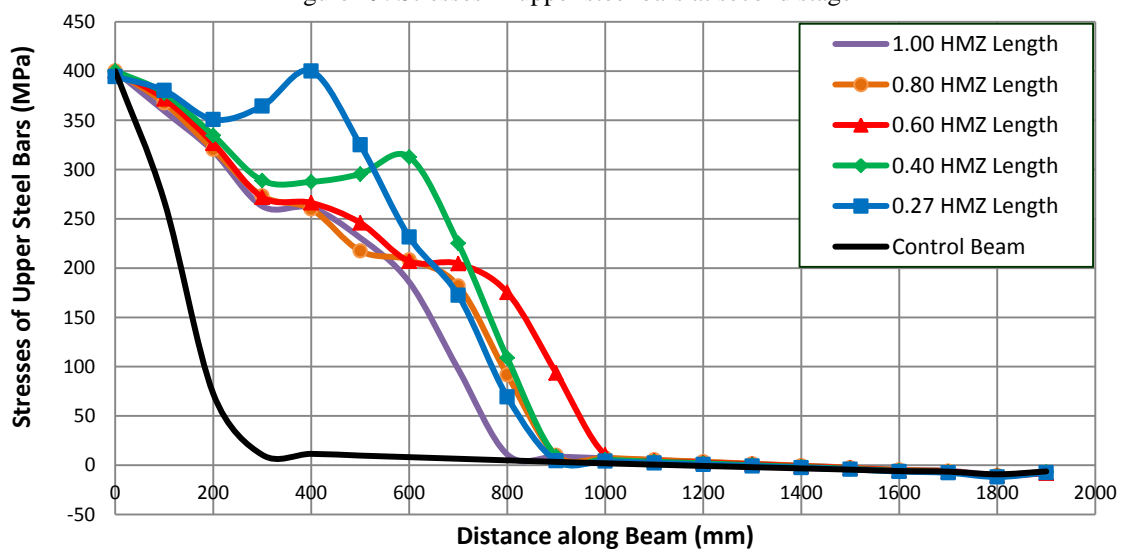


Figure 20. Stresses in upper steel bars at steel yield

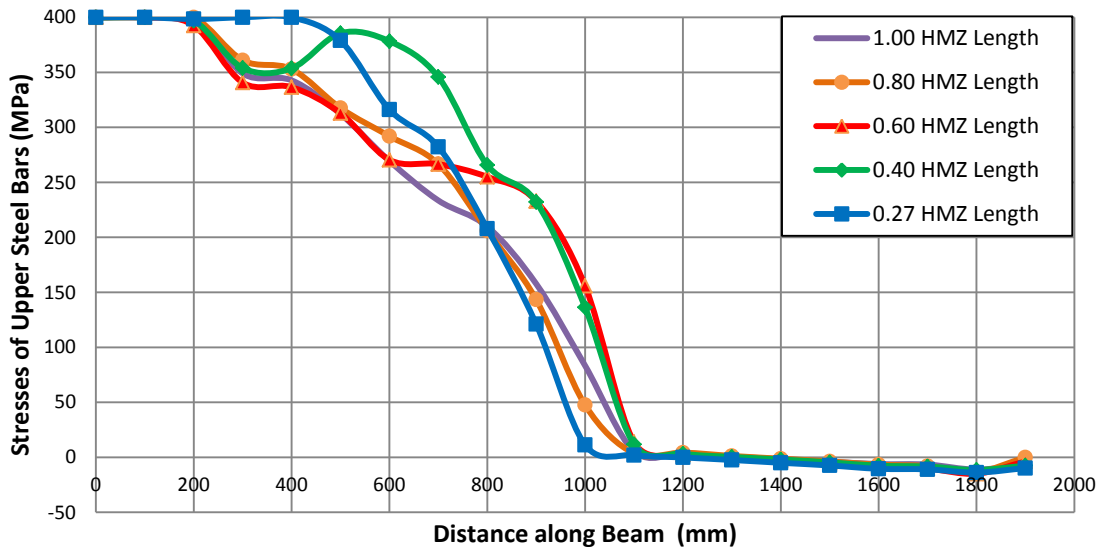


Figure 21. Stresses in upper steel bars at fourth stage

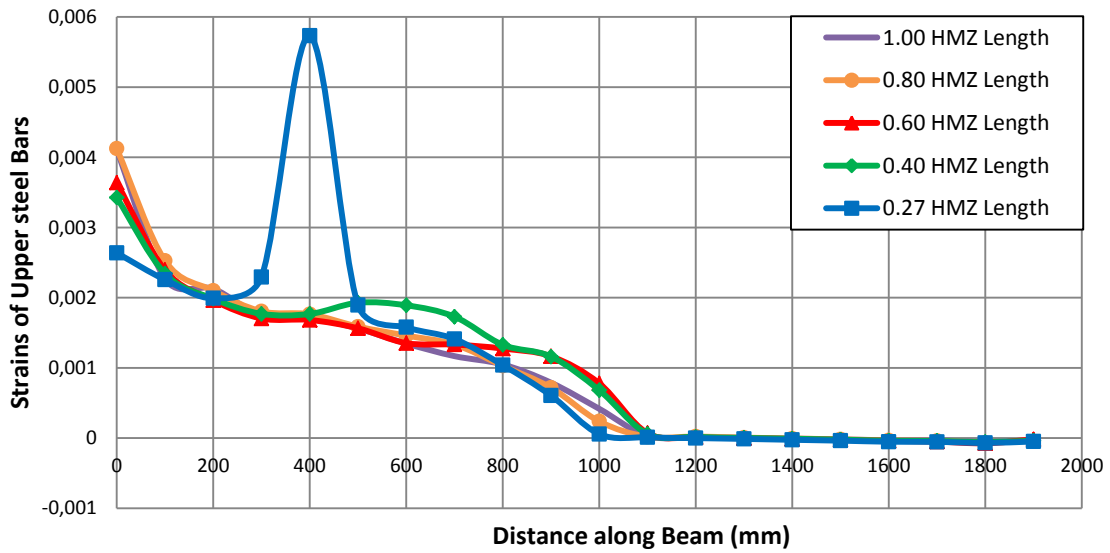


Figure 22. Strains in upper steel bars at fourth stage

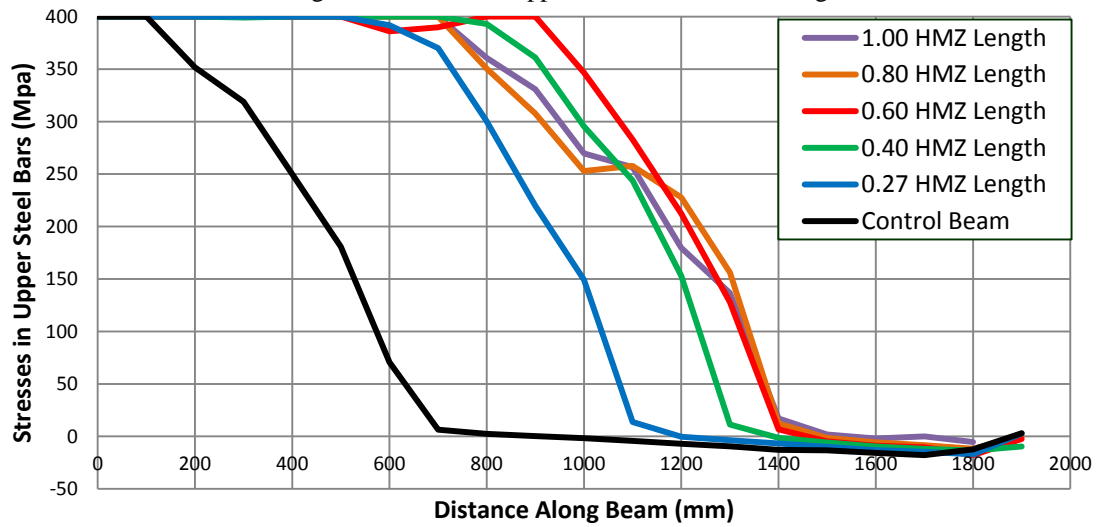


Figure 23. Stresses in upper steel bars at failure

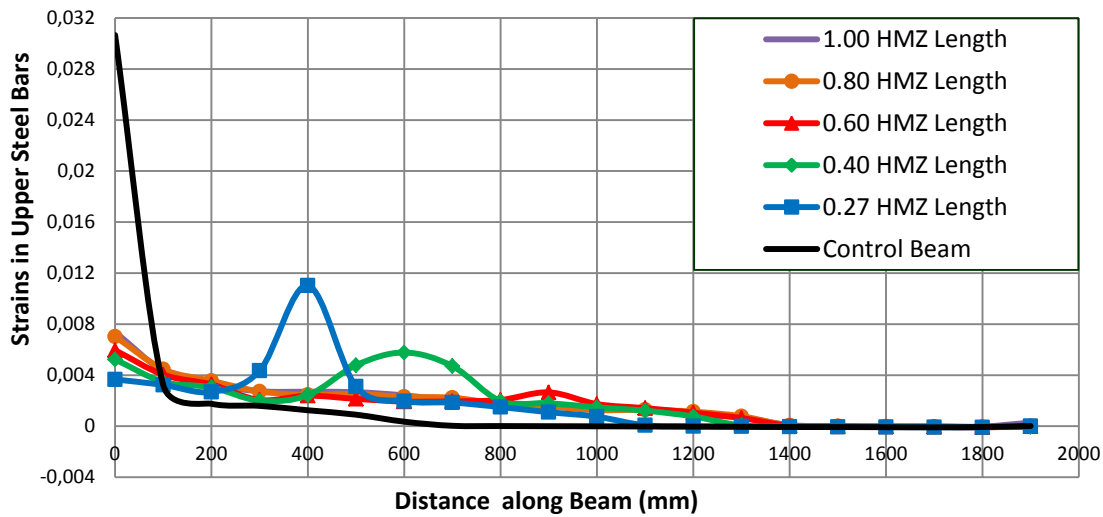


Figure 24. Strains in upper steel bars at failure

According to the results, the following may be added to what previously concluded:

1. Stresses are not affected by the presence of CFRP laminates until first crack of concrete
2. Stresses (strains) of steel bars are of maximum value at mid-support and decrease gradually as a general along their length.
3. For strengthening length of 400mm, stresses and strains of upper steel bars increase suddenly and sometimes dramatically at the end of CFRP Laminates. This happens to some extent with 600mm CFRP length.
4. Stresses/strains for CFRP lengths 1200 and 1500mm are close, especially after yielding.
5. Increasing the lengths of CFRP laminates improves strains distribution and, to some extent, stresses distribution of upper steel bars. So, it improves the utilizing of upper steel bars.
6. According to the behavior of upper steel bars the optimum CFRP length is ($L_{CFRP} = 0.8L_{HMZ}$), while the minimum length has to be more than $0.4L_{HMZ}$.

3.3.6 Moment Redistribution

Redistribution of moments between both sagging and hogging moments allows good utilizing of the beam capacity. Moment redistribution factor (β) is defined as:

$$\beta = \left(\frac{M_{FE} - M_E}{M_E} \right) \times 100 \quad \% \quad (1)$$

Where M_{FE} is the bending moment calculated from FE results at failure (using both failure loads and their corresponding reactions), and M_E is the failure bending moment calculated elastically due to applied loading at failure. Figure 25 shows diagrams for the control beam (BC) and the strengthened beams BS1, BS2, BS3, BS4 and BS5 with CFRP lengths 400, 600, 900, 1200 and 1500 mm, respectively, for both M_{FE} and M_E . Only one span is drawn due symmetry. Table 2 contains the absolute values of the moment redistribution factor (β) for the different beams. Increasing the length of CFRP laminates decreases the absolute value of the moment redistribution factor (β). This means that increasing CFRP length will lead to formation of a plastic hinge. Since moment redistribution factor (β) in the span is less than this of the mid-support (by about 50%), the plastic hinge will form at the location of maximum span (sagging) moment. As a result, the increasing of FE sagging (span) moment is slight which allows the mid-support (hogging) moment to increase clearly till failure, especially when compared with the values of the control (unstrengthened) beam. This process is called moment redistribution. This means that increasing CFRP lengths improves the utility of moment capacity of the beam either sagging or hogging.

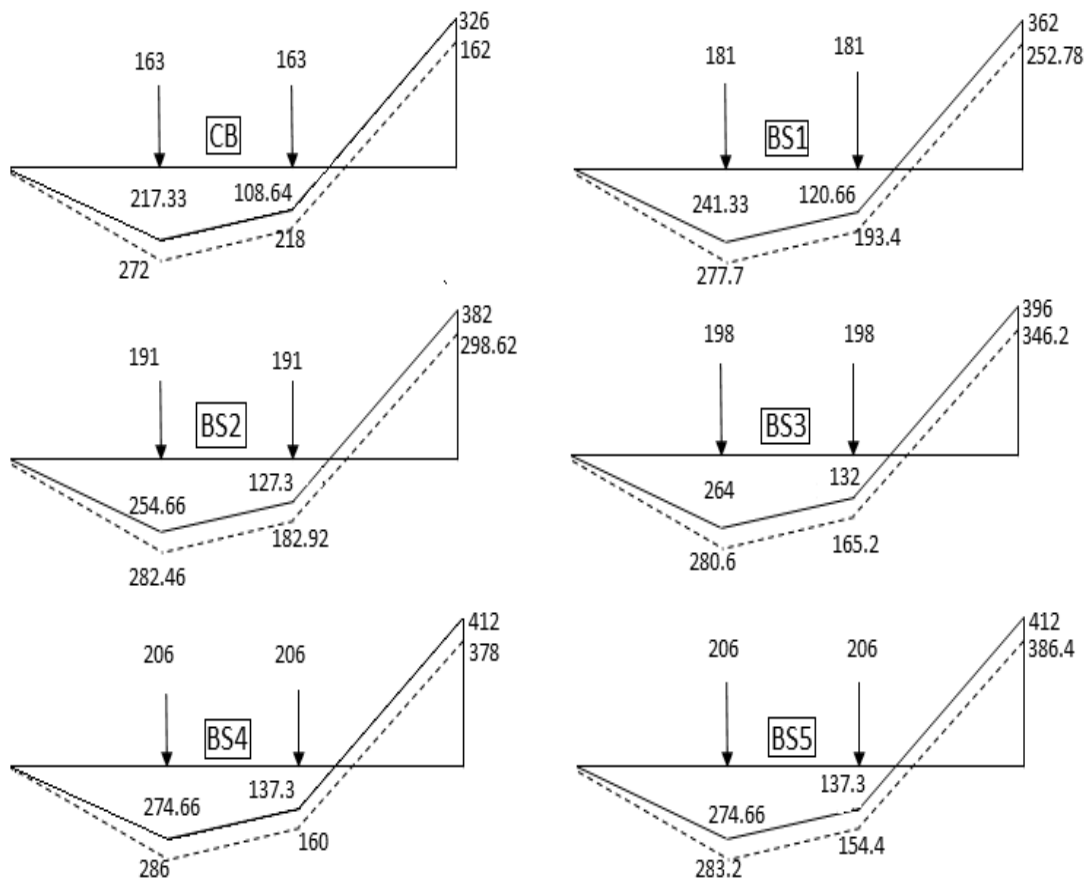


Figure 25. Redistribution of moments: (M_E—) and (M_{FE}- - -) moments diagrams

Table 2. Values of moment redistribution factor (β)

Beam	P _u (KN)	Reactions (KN)		Mid-Support			Span		
		Mid-Support	End Support	M _{FE} (KN.m)	M _E (KN.m)	β (%)	M _{FE} (KN.m)	M _E (KN.m)	β (%)
BC	326	189.91	136.09	162.00	326	50.31	272.18	217.00	25.43
BS1	362	223.13	138.87	252.78	362	30.17	277.70	241.33	15.07
BS2	382	240.77	141.23	298.62	382	21.83	282.48	254.66	10.92
BS3	396	253.70	142.30	346.20	396	14.33	280.60	264.00	6.29
BS4	412	268.98	143.02	378.00	412	8.25	286.00	274.66	4.13
BS5	412	270.33	141.67	386.40	412	6.21	283.20	274.66	3.11

3.3.7 Energy Dissipation and Ductility

Figure 26 shows definition of the energy dissipated by any of the studied beams at the yielding of upper steel bars (E_y) and at failure (E_u). Also, it shows deflections at both yield (Δ_y) and failure (Δ_u). Ductility index (μ_D) and energy dissipation index (μ_E) are used to measure both ductility and energy dissipation, respectively, and they are defined as:

$$\mu_D = \frac{\Delta_u}{\Delta_y} \quad (2)$$

$$\mu_E = \frac{E_u}{E_y} \quad (3)$$

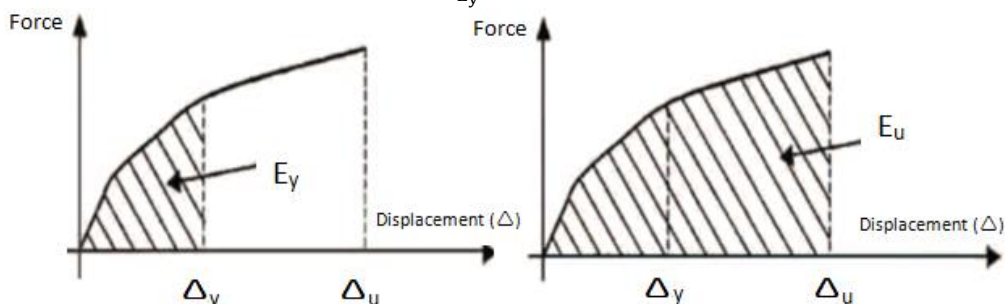


Figure 26. Definitions of ductility and energy dissipation

Table 3 shows the values of both ductility and energy dissipation indexes for the studied beams. Increasing the length of CFRP laminate increases both ductility index and energy dissipation index, which means a very good utilizing of the beam after yielding of upper steel bars. Both capacity (strength) and ductility of the strengthened beam increase very much with increasing of the CFRP laminate length.

Table 3 Values of ductility index μ_D and energy dissipation index μ_E

Beam	(Δy) m	(Δu) mm	$\mu_D = \frac{\Delta u}{\Delta y}$	Increase over BC (%)	(E_y) KN.mm	(E_u) KN.mm	$\mu_E = \frac{E_u}{E_y}$	Increase over BC (%)
BC	11.2	13.8	1.232	-----	2408.756	3243.356	1.346	-----
BS1	10.8	14.9	1.380	11.970	2434.412	3894.012	1.600	18.796
BS2	10.8	18	1.667	35.266	2468.156	5117.756	2.073	53.994
BS3	10.8	20.1	1.861	51.047	2563.796	6125.696	2.389	77.448
BS4	10.1	23.5	2.327	88.836	2314.316	7486.716	3.235	140.252
BS5	10.1	24.8	2.455	99.283	2314.316	7988.516	3.452	156.355

3.3.8 Shear Stresses at the Interface between RC-Beam and CFRP Laminate

Figure 27 shows the distribution of shear stresses in the bond layer between beam and CFRP along length of laminates. Increasing length leads to decreasing of bond stresses which means that the probability of debonding decreases with increasing CFRP length. Table 4 shows modes of failure for the different CFRP lengths which insures this result.

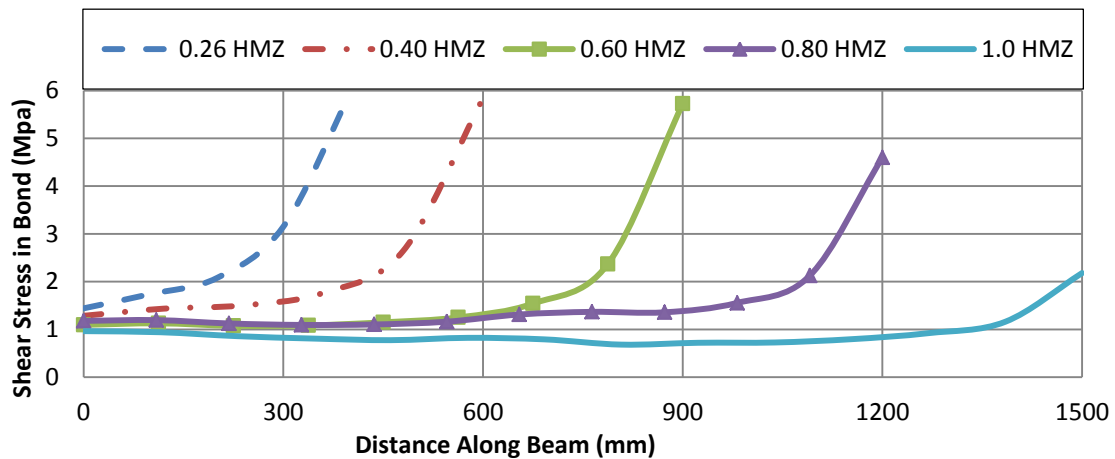


Figure 27. Shear stress in bond layer

Table 4. Failure modes

Beam	CFRP Length	Failure Mode
BC	-----	Flexure at Mid-Support
BS1	0.27 HMZ	CFRP Debonding
BS2	0.40 HMZ	CFRP Debonding
BS3	0.60 HMZ	CFRP Debonding
BS4	0.80 HMZ	Flexure at Mid-Support
BS5	1.0 HMZ	Flexure at Mid-Support

According to results of the table, an additional definition for the optimum CFRP length can be put as the minimum CFRP length that does not allow the debonding between the CFRP laminate and the surface of the RC beam. As a conclusion, CFRP length of 1200mm (0.80 L_{HMZ}) is the optimum CFRP length for the strengthened beam of upper reinforcement of 4 bars of diameter 12mm and CFRP thickness of 0.9mm.

3.3.9 Optimum (Effective) Length

The effective or optimum length (L_{Opt}) is the length beyond it no improvement in the behavior of the strengthened beam is achieved. Also, it can be added that it is the length which does not allow debonding of CFRP laminate, and hence the failure mode will be only according to either cracking or crushing of the concrete. In the previous sections, the optimum or effective length was calculated for a certain percentage of reinforcement and a constant CFRP thickness. However, it is logic and expected for this length to change with change of both

reinforcement percentage and CFRP thickness. For this reason, the previous parametric study was repeated for different thicknesses and different percentage ratios of reinforcement as follows. Three CFRP thicknesses were studied; 0.9, 1.2, and 1.6mm. For each of these thicknesses, three diameters of the upper reinforcements were used; 12, 16, and 18mm. For each of these diameters, six lengths as an average in the range from 600 to 1500mm were studied. This means that to complete this extensive parametric study, a total number of 55 FE models of RC T-section beams strengthened with CFRP laminates.

Tables 5 to 13 show the results of this parametric study bearing in mind that the optimum length was chosen according to two conditions:

a. Values of both ultimate loading and maximum deflection are considered related to the optimum length as far as no significant increasing is found with the increasing of CFRP length. In other words, these values have to be approximately equal to the following ones.

b. No debonding failure may occur if CFRP length \geq the optimum one.

Results show an excellent agreement between both conditions. Also, additional two conditions were found at optimum length:

a. CFRP stresses are approximately maximum.

b. Position of zero moment will remain constant for CFRP lengths \geq the optimum one.

Finally, since steel reinforcement was modeled as elastoplastic material ($\sigma_y = \sigma_u$), the stresses in steel reinforcement at failure will be equal for all the models and equals the yield (failure) stress of the steel bars. So, they are not concluded in the following results of the parametric study.

Table 5. Optimum length for thickness 1.6mm and reinforcement diameter 12mm

CFRP Length (mm)	Ultimate Load (KN)	Deflection (mm)	Max. CFRP Stresses (MPa)	Distance of zero-Moment	Failure Mode
600	388	17.7	-----	-----	Debonding
900	418	22.3	-----	-----	Debonding
1000	436	29.4	-----	-----	Debonding
1200	450	33.5	1060	1600	Debonding
1300	462	34.5	1110	1800	Debonding
1320	468	35.99	1160	1800	Flexure
1500	470	36.8	1164.4	1800	Flexure

Table 6. Optimum length for thickness 1.6mm and reinforcement diameter 16mm

CFRP Length (mm)	Ultimate Load (KN)	Deflection (mm)	Max. CFRP Stresses (MPa)	Distance of zero-Moment	Failure Mode
1000	448	23.1	820.2	1700	Debonding
1100	458	25.6	889	1750	Debonding
1150	470	27.9	940	1800	Flexure
1200	470	28.1	948.2	1800	Flexure
1500	470	27.9	959.05	1800	Flexure

Table 7. Optimum length for thickness 1.6mm and reinforcement diameter 18mm

CFRP Length (mm)	Ultimate Load (KN)	Deflection (mm)	Max. CFRP Stresses (MPa)	Distance of zero-Moment	Failure Mode
900	496	28.23	-----	-----	Debonding
1000	502	31.9	970.9	1700	Debonding
1020	508	33.9	1085	1800	Flexure
1100	508	33.44	1093.5	1800	Flexure
1200	506	33.58	1102.41	1800	Flexure
1500	508	32.2	-----	-----	Flexure

Table 8. Optimum length for thickness 1.2mm and reinforcement diameter 12mm

CFRP Length (mm)	Ultimate Load (KN)	Deflection (mm)	Max. CFRP Stresses (MPa)	Distance of zero-Moment	Failure Mode
900	-----	-----	-----	1500	Debonding
1100	414	23.7	867.72	1600	Debonding

1200	420	25.6	1062	-----	Debonding
1250	430	30.9	1153	-----	Debonding
1270	446	36.6	1350.2	1800	Flexure
1300	446	36.2	1396.4	1800	Flexure
1500	448	36.4	-----	-----	Flexure

Table 9. Optimum length for thickness 1.2mm and reinforcement diameter 16mm

CFRP Length (mm)	Ultimate Load (KN)	Deflection (mm)	Max. CFRP Stresses (MPa)	Distance of zero-Moment	Failure Mode
600	406	16.9	-----	-----	Debonding
900	430	20.6	877.68	1700	Debonding
1000	444	23	1006.6	1800	Debonding
1100	458	27.8	1183.52	1800	Flexure
1200	460	28.3	1190.8	1800	Flexure
1500	462	28.9	-----	-----	Flexure

Table 10. Optimum length for thickness 1.2mm and reinforcement diameter 18mm

CFRP Length (mm)	Ultimate Load (KN)	Deflection (mm)	Max. CFRP Stresses (MPa)	Distance of zero-Moment	Failure Mode
600	430	18.68	-----	-----	Debonding
900	450	23.8	942.22	1600	Debonding
970	480	26.98	1152.1	1800	Flexure
1000	480	26.96	1180.	1800	Flexure
1200	482	27.5	1200	1800	Flexure
1500	484	28.34	-----	-----	Flexure

Table 11. Optimum length for thickness 0.9mm and reinforcement diameter 12mm

CFRP Length (mm)	Ultimate Load (KN)	Deflection (mm)	Max. CFRP Stresses (MPa)	Distance of zero-Moment	Failure Mode
400	362	15	640.42	1200	Debonding
600	382	18	856.9	1400	Debonding
900	396	20.3	1095	1500	Debonding
1100	405	23.65	1122.35	1500	Debonding
1200	412	24.05	1302.4	1600	Flexure
1500	412	24.8	1326.7	1600	Flexure

Table 12. Optimum length for thickness 0.9mm and reinforcement diameter 16mm

CFRP Length (mm)	Ultimate Load (KN)	Deflection (mm)	Max. CFRP Stresses (MPa)	Distance of zero-Moment	Failure Mode
400	392	16.392	-----	-----	Debonding
600	410	19.75	-----	-----	Debonding
900	428	23.4	1164.6	1500	Debonding
1000	438	24.7	1278.2	1500	Debonding
1050	452	29.5	1377.1	1600	Flexure
1200	452	29.55	1401.8	1600	Flexure
1500	454	29.6	1404	1600	Flexure

Table 13. Optimum length for thickness 0.9mm and reinforcement diameter 18mm

CFRP Length (mm)	Ultimate Load (KN)	Deflection (mm)	Max. CFRP Stresses (MPa)	Distance of zero-Moment	Failure Mode
600	434	24.6	1000.38	1500	Debonding
800	446	29.38	-----	-----	Debonding
900	492	36	1488.8	1600	Flexure
1200	492	35.43	1515.7	1600	Flexure
1500	492	34.43	1518.236	1600	Flexure

3.3.10 Required CFRP Length (L_{req})

Figure 28 shows the elastic bending moment diagram of the original designed unstrengthened beam (upper reinforcement 4-bars- ϕ 24mm) for one span of the studied symmetric beam. Three horizontal lines, corresponding to the capacities of the unstrengthened beams with the reduced upper reinforcement are drawn; 4-bars- ϕ 12mm, 4-bars- ϕ 16mm and 4-bars- ϕ 18mm. These straight lines intersect with the elastic bending diagram at distances 1105, 818, and 625mm, respectively, measured from the mid-support. These distances represent the lengths of CFRP laminates, (L_{req}), required to recover the capacity of the original designed control beam (BC0).

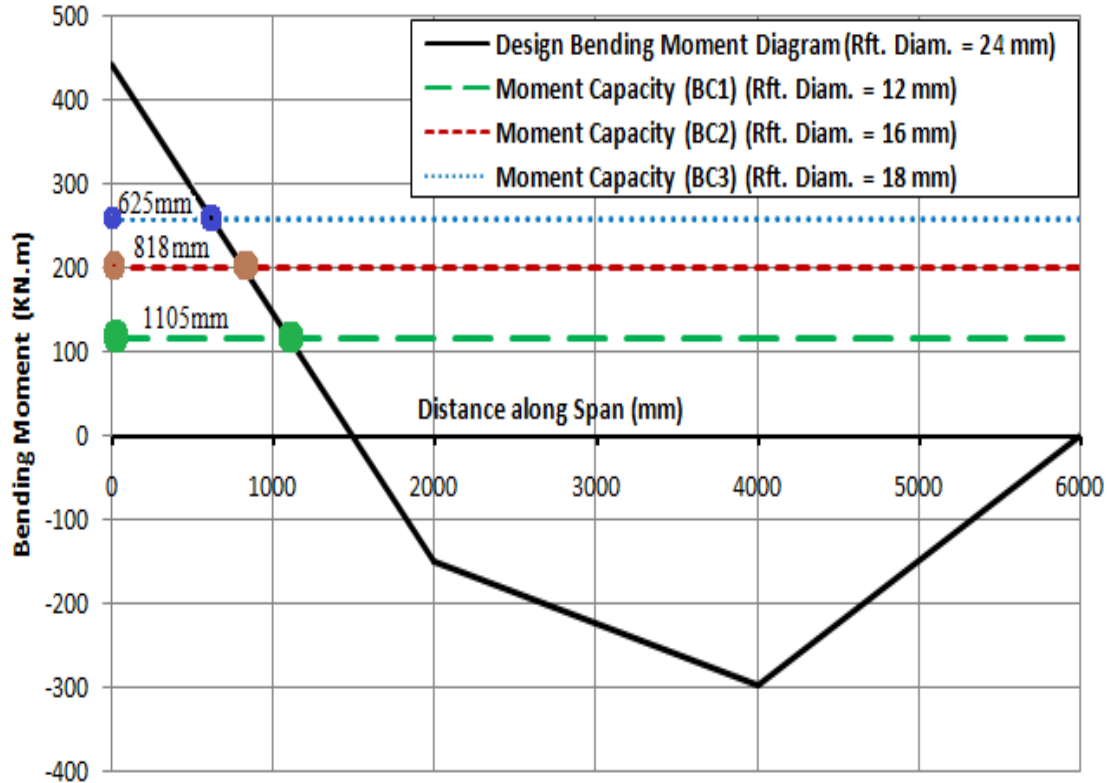


Figure 28. Required CFRP theoretical lengths from the elastic bending moment

3.3.11 Optimum Length vs. Required Length

Table 14 shows a comparison between the optimum length calculated using FE results (L_{opt}) as mentioned before and the required length calculated theoretically (L_{req}).

Table 14. Theoretical and FE optimum lengths

ϕ m	L_{Req}	Thickness of CFRP Laminates (mm)								
		$t_{CFRP} = 1.6$			$t_{CFRP} = 1.2$			$t_{CFRP} = 0.9$		
		L_{Opt}	$L_{Opt} - L_{Req}$	$\frac{L_{Opt}}{L_{Req}}$	L_{Opt}	$L_{Opt} - L_{Req}$	$\frac{L_{Opt}}{L_{Req}}$	L_{Opt}	$L_{Opt} - L_{Req}$	$\frac{L_{Opt}}{L_{Req}}$
12	1105	1320	215	1.195	1270	165	1.149	1200	95	1.086
16	818	1150	332	1.406	1100	282	1.345	1050	232	1.284
18	625	1020	395	1.632	970	345	1.552	900	275	1.44

Figure 29 shows the relation between the effect of the reinforcement (Rft.) in the form of (design Rft. / reduced Rft.) and the CFRP length in the form of (optimum length / required length) for different thicknesses. It is shown that, for constant reinforcement, increasing the thickness of CFRP laminate increases the value (L_{opt}/L_{req}). Also, for constant (L_{opt}/L_{req}), increasing the thickness means a decreasing in the negative reinforcement. Finally, for the same thickness, increasing the ratio (L_{opt}/L_{req}) means an increasing in the negative reinforcement.

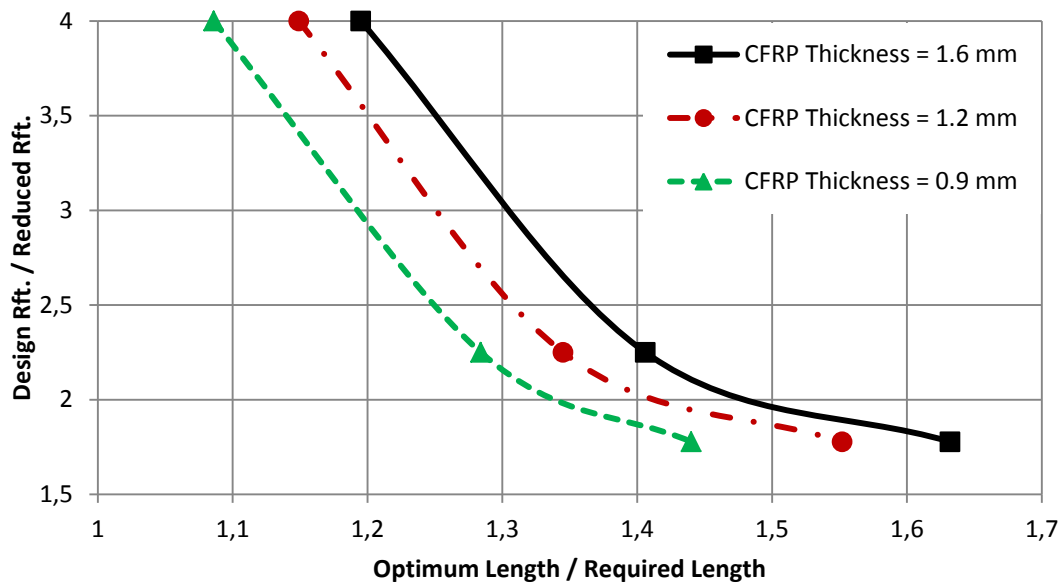


Figure 29. Change of reinforcement vs. CFRP length

3.3.12 Anchorage CFRP Length

According to the results shown in Table 14:

- FE results are always more than that calculated theoretically.
- The difference between the two lengths calculated theoretically (L_{Req}) or using FE (L_{Opt}) is the length that expresses the anchorage length needed theoretically to make the strengthened beam behaves as full bonded beam between the CFRP laminates and the concrete surface.
- This anchorage length (L_{Anchor}) is in the range from 95 to 395 mm with an average value equals 245 mm while in ECP-208; Egyptian Code for Using CFRP in Fields of Construction, it is the biggest between 150 mm and the depth of the concrete section.
- The ratio between CFRP lengths calculated using ANSYS (L_{Opt}) or using theoretical calculation (L_{Req}) is in the range between 1.1 and 1.6.
- This ratio expresses the ratio between the optimum length (effective length including the anchorage length) and the effective or required length (without anchorage length).
- Table 15 shows the values of anchorage lengths (L_{Anchor}) for the different cases and its ratio with beam depth ($d=650\text{mm}$).

Table 15. Anchorage lengths related to the beam depth

ϕ m	Thickness of CFRP Laminates (mm)					
	$t_{CFRP} = 1.6$		$t_{CFRP} = 1.2$		$t_{CFRP} = 0.9$	
	L_{Anchor}	$\frac{L_{Anchor}}{d}$	L_{Anchor}	$\frac{L_{Anchor}}{d}$	L_{Anchor}	$\frac{L_{Anchor}}{d}$
12	215	0.33	165	0.25	95	0.15
16	332	0.51	282	0.43	232	0.36
18	395	0.61	345	0.53	275	0.42

- The ratio ($\frac{L_{Anchor}}{d}$) is in the range from 0.15 to 0.61 with an average value of 0.38 while it equals 0.5 in the American Standards and 1.0 in the Egyptian Code.
- As a recommendation, anchorage length has to be taken as the maximum of 250mm and the beam depth.

2. Conclusions

This paper examines the effect of CFRP length upon the behavior of RC T-beams strengthened either in the hogging moment zones. Also, both optimum and anchorage CFRP lengths are calculated. According to the results, the following can be concluded:

- Effect of strengthening with CFRP laminates begins just after first crack of concrete.
- Increasing the lengths of CFRP laminates increases the capacity of the beam in the hogging moment and the corresponding deflection.

- Stresses (strains) of CFRP laminates are of maximum value at mid-support and decrease gradually along their length.
- Maximum contribution of CFRP laminates occurs after yielding of upper steel bars.
- Increasing length of CFRP laminate maximizes its benefits and decrease concentration of stresses at its end.
- Stresses (strains) of steel bars are of maximum value at mid-support and decrease gradually as a general along their length.
- Increasing lengths of CFRP laminates improves strains distribution and, to some extent, stresses distribution of upper steel bars. So, it improves the utilizing of upper steel bars.
- Increasing the length of CFRP laminates improves, very much, the redistribution of moments between sagging and hogging moments. This means much more utilizing of the moment capacity of the beam either sagging or hogging.
- Increasing CFRP length increases both ductility and energy dissipation of the beam.
- Increasing CFRP length decreases the bond stresses. This means that the probability of debonding decreases with increasing of CFRP length.
- Optimum length of CFRP laminate is the length that covers the lack between the actual capacity of RC section and the required (or design) capacity of the beam, including the anchorage length of the CFRP laminate.
- Anchorage length has to forbid the debonding between both CFRP laminates and the concrete surfaces.
- The optimum length can be taken between 1.1 and 1.6 of the required length calculated theoretically, according to the actual percentage of upper reinforcement.
- Anchorage length has to be taken as the maximum of 250mm and the beam depth.

References

- El-Mogy M., El-Ragaby A., and El-Salakawy E.: Experimental testing and finite element modeling on continuous concrete beams reinforced with fibre reinforced polymer bars and stirrups. *Canadian Journal of Civil Engineering*, 40 (11), 1091–1102, November, (2013).
- El-Refaie S. A., Ashour A. F. and Garrity S. W.: Sagging and Hogging Strengthening of Continuous Reinforced Concrete Beams Using Carbon Fiber-Reinforced Polymer Laminates. *ACI Structural Journal*, 100 (4), 446-453, July-August, (2003).
- Maghsoudi A. A. and Bengar H. A.: Moment redistribution and ductility of RHSC continuous beams strengthened with CFRP. *Turkish Journal of Engineering and Environmental Sciences* (<http://journals.tubitak.gov.tr/engineering/issues/muh-09-33-1/muh-33-1-5-0901-6.pdf>), 33, 45-59, (2009).
- Saleh A. R. and Barem A. A. H.: Experimental and Theoretical Analysis for Behavior of R.C. Continuous Beams Strengthened by CFRP Laminates. *Journal of Babylon University (Iraq) - Engineering Sciences*, 21 (5), 1555-1567, (2013).
- Saribiyik A. and Caglar N.: Flexural strengthening of RC Beams with low-strength concrete using GFRP and CFRP. *Journal of Structural Engineering and Mechanics*, 58 (5), 825-845, June, (2016).
- Rahman M. M. and Rahman M. W.: Simplified method of strengthening RC continuous T beam in the hogging zone using carbon fiber reinforced polymer laminate - A numerical investigation. *Journal of Civil Engineering Construction Technology* (<http://www.academicjournals.org/JECET>), 4 (6), 174-183, June, (2013).
- Iesa W. M., Alferjani M. B. S., Ali N. and AbdulSamad A. A.: Study on Shear Strengthening of RC Continuous Beams with Different CFRP Wrapping Schemes. *International Journal of Integrated Engineering (Issue on Civil and Environmental Engineering)* (<http://penerbit.uthm.edu.my/ojs/index.php/ijie/article/view/207>), 2 (2), 35-43, (2010).
- Lu X. Z., Ten J. G., Ye L. P., Jaing J. J.: Bond-slip models for FRP sheets/plates bonded to concrete. *Journal of Engineering Structures*, 24 (5), 920-937, (2005).
- Aiello M. A. and Ombre, L.: Moment Redistribution in Continuous Fiber-Reinforced Polymer-strengthened Reinforced Concrete Beams. *ACI Structural Journal*, 158-166, March-April, (2011).
- In press article:
- Mohie Eldin M, Tarabia A. M. and Hasson R. F.: CFRP Strengthening of Continuous RC T-Beams at Hogging Moment Zone across the Flange. Accepted in *Journal of Structural Engineering and Mechanics*, Techno-press, 2018 (In Press).
- Tarabia A. M., Mohie Eldin M and Hasson R. F.: Failure Modes of Continuous Reinforced Concrete T-Beams Strengthened Using CFRP Laminates. Accepted in 'Proceeding of the International Conference on Advances in Civil, Structural and Mechanical Engineering, Antalya, Turkey', October, 2017 (In press).
- Shrestha U. S.: Modified Composite Application to Improve Strength and Ductility of Structural Components. MSc Dissertation, College of Graduate Studies, The University of Toledo, Ohio, United States, (2014).
- ANSYS: ANSYS Help. Release 15 (2013).

- Taerwe L., Vasseur L. and Matthys S.: External strengthening of continuous beams with CFRP. in 'Concrete Repair, Rehabilitation and Retrofitting II' Alexander et al (eds), Taylor & Francis Group, ISBN 978-0-415-46850-3, London, 43-53, (2009).
- Thorenfeldt E., Tomaszewicz A. and Jensen J.: Mechanical Properties of High Strength Concrete and Application to Design. in 'Proceedings of the Symposium: Utilization of High-Strength Concrete, Stavanger, Norway', 149–159, June, (1987).
- Sakr M. A., Khalifa T. M. and Mansour W. N.: External Strengthening of RC Continuous Beams Using FRP Plates: Finite Element Model. In 'Proceeding of the Second International Conference on Advances in Civil, Structural and Mechanical Engineering- CSM 2014', ISBN: 978-1-63248-054-5, 168-174, (2014).
- ECP-203: Egyptian Code of Practice for the Design and Implementation of Reinforced Concrete Structures (2007).
- ECP-208: Egyptian Code for the Design Principles and Implementation Requirements of Using CFRP in Fields of Construction (2005).